Characterization of the age and nature of the lithosphere in the Tsumkwe region, Namibia

K.O. Hoal[1], B.G. Hoal[2], W.L. Griffin[3, 4] and R.A. Armstrong[5]

[1]*Hazen Research Inc., 4601 Indiana St., Golden, Colorado 80403, USA*
[2]*Society of Economic Geologists (SEG), 7811 Shaffer Parkway, Littleton, CO 80127, USA*
[3]*Key Centre for Geochemical Evolution and Metallogeny of Continents, Macquarie University, NSW 2109, Australia*
[4]*CSIRO Division of Exploration and Mining, Box 136, North Ryde, NSW 2113, Australia*
[5]*Research School of Earth Sciences, The Australian National University, Canberra, ACT 0200, Australia*

Diamond exploration conducted by Rio Tinto Namibia in the Tsumkwe region of northeast Namibia from 1994 to 1996 produced significant enough populations of kimberlitic indicator minerals, particularly G10 garnets, to warrant further study of the poorly exposed basement. Although representing a geochemically diverse population, most of the garnets studied appear to have been derived from a mantle with a cratonic geotherm, a diamond window of 900° to 1250°C, and a lithosphere thickness of at least 190 km. G10 garnets are moderately abundant and fall within the diamond window. Zircons from basement megacrystic granite produced a 206Pb/238U magmatic crystallization age of 852 ± 11 Ma, and zircons from fine-grained granitic gneiss produced a crystallization age of 2022 ± 15 Ma with lead loss, possibly relating to a metamorphic event, at about 970 Ma. Combined, these results indicate the presence of a stabilized continental segment, established by at least 2.0 Ga, which included mantle with some Archean-like characteristics at the time of kimberlite eruption. This portion of the lithosphere may have been a thinned southern edge of the Congo craton.

Introduction

This study focuses on the eastern part of the Otjozondjupa political region, referred to herein as the Tsumkwe region. Despite being largely covered by Kalahari sediments, the area has long been considered to be prospective for diamondiferous kimberlites and lamproites, occurring as it does across the border from significant kimberlite occurrences in Botswana. The discovery of at least three diamonds in soil samples (Rio Tinto Namibia, unpub. data, 1995) has further created exploration interest in the region. Reconnaissance indicator mineral sampling was conducted by De Beers from 1978 to 1984 and targeted a large region in northern and eastern Namibia, narrowing down to the northeastern area centered on the village of Tsumkwe. During the course of that program, De Beers uncovered the four Sikereti kimberlites approximately 60 km north of Tsumkwe. Although barren of diamonds, the presence of the Sikereti kimberlite cluster indicated the potential for other kimberlites in the region. Important indicator mineral anomalies were also discovered in the neighboring Tsumkwe area, however due to political and other conditions at the time these anomalies were not followed up.

The current project grew out of regional diamond exploration work conducted by Rio Tinto Namibia, Pty Ltd. from 1994 to 1996. During that time, several hundred loam samples were collected from an area extending from the Gam region in the south to the Sikereti kimberlites in the north, and from the Botswana border in the east to some 40 km west of Tsumkwe. Rio Tinto also had most of that area covered with airborne geophysics. In the course of the program, hundreds of mantle-derived indicator minerals indicative of the presence of kimberlites or lamproites were taken from the loam samples. Approximately 20 percent of these minerals were so-called G10 (Cr-rich, subcalcic) garnets that are, by analogy to diamond-inclusion garnets, indicative of the possible diamond potential of a kimberlite (Gurney and Zweistra, 1995). Work by Rio Tinto and by De Beers on surface textures of indicator minerals further supported local source regions (3 to 5 km) for the garnets that were studied (De Beers, unpub. data, 1978, 1984; Rio Tinto, unpub. data, 1994, 1996).

In this paper, we describe results of geochemical and geochronological studies on mantle-derived garnets and basement rocks from the Tsumkwe region. The work, which was sponsored by Rio Tinto Namibia, was conducted in order to gain information on the nature and age of the lithosphere in the region. The geochemical studies of garnets are particularly important in identifying mantle geotherms and the diamond potential of the region at the (unknown) time of kimberlite emplacement. The basement ages are significant contributions to the small database of this large, sand-covered portion of the country.

Geologic framework

Much of the bedrock geology of the Tsumkwe region has remained unknown and mostly inferred because much of northeast N3Agriculture, Water and Rural Development (Gam region), and the Geological Survey of Botswana (northwest Botswana) have further contributed to the understanding of major geological belts and structures in the area.

From regional geologic mapping and geophysical surveys (Eberle *et al.*, 1995; 1:1 000 000 Geological Map of Namibia, 1980), a northeast-trending belt of pre-Damara basement crosses northeast Namibia and extends through the Tsumkwe region and into Botswana. Where exposed in the east of the Tsumkwe area, these rocks consist of fine-grained granitic gneiss, amphibolite, and coarse megacrystic granite. They have been correlated previously with the ca. 1800 m.y. old Grootfontein Metamorphic Complex (Balfour *et al.*, 1985). Between the villages of Tsumkwe and Gam,

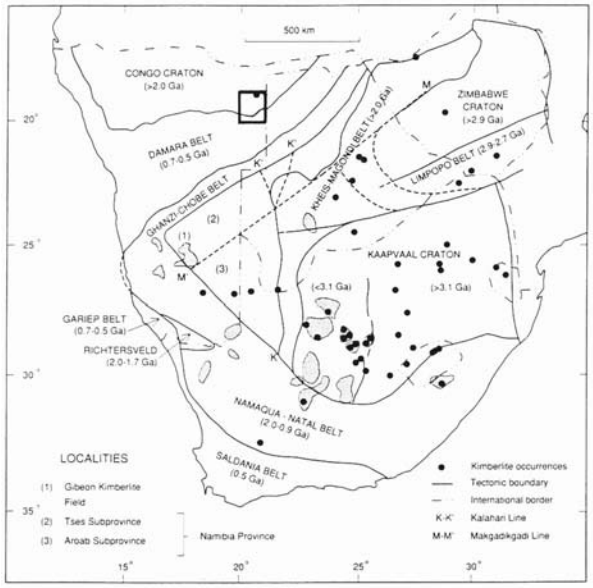

Figure 1A: Map of southern Africa (after Hoal et al., 1995) showing major structural boundaries and the Tsumkwe region (outlined).

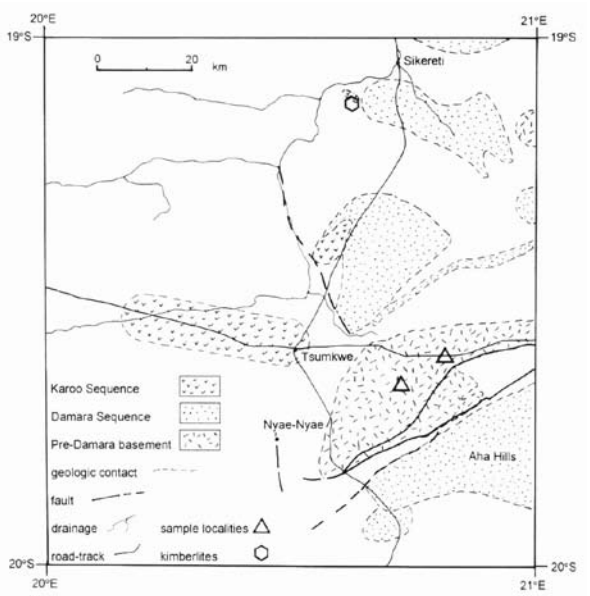

Figure 1B: Geologic sketch map of the Tsumkwe area showing the distribution of outcrop and suboutcrop beneath the Kalahari cover (blank areas; modified from the Geological map of Namibia, 1980). Locations of geochronology samples and the Sikereti kimberlites are also shown. Indicator minerals were recovered from loam samples taken from the central part of the region shown, from west of Nyae-Nyae and north of Tsumkwe to the Botswana border (longitude 21□E).

to the south, the belt appears to be truncated or to flex downwards, as its highly magnetic character terminates in a series of covered, northeast-trending linear features or fault zones (B. Corner, pers. comm. 1995; T. Smalley, pers. comm. 1995). Southeast of this region is a magnetically relatively quiet zone considered to be composed of Damara-age sediments. The Damara rocks are exposed in the Aha Hills and consist largely of sandstones and carbonates correlated with the Nosib and Otavi Groups (Balfour *et al.*, 1985).

Overlying the basement rocks in the Tsumkwe area and in blocks and segments farther south are the magnetically distinctive Karoo rocks which, although largely unexposed, are presumed to consist of volcanic and sedimentary rocks. Several large, distinctive circular structures are prominent in the geophysical pattern of the Karoo sequence. Their origin and significance are as yet unknown (Rio Tinto Namibia, unpub. data, 1995). The Karoo sequence was apparently deposited in the vicinity of a basement high, as it rests directly upon the pre-Damara basement. The broad band of the ca. 1500 km-long Okavango dyke swarm, which trends southeast across the continent from southern Angola to eastern South Africa, signaled late Karoo uplift and mantle upwelling reflecting a failed arm to a triple junction (Uken and Watkeys, 1997). The Sikereti kimberlites occur along the southern edge of the dyke swarm and may have been emplaced at that time, as they appear to contain xenoliths of Karoo rocks. Alternatively, they may have been emplaced in early Kalahari time, since they contain xenoliths of sedimentary rocks that resemble Kalahari stratigraphy but which may also be Karoo rocks (Balfour *et al.*, 1985).

The Kalahari sequence is locally up to 200 m or more thick. The lower Kalahari units record fluvial drainage off basement highs and contain the majority of the kimberlite indicator minerals as a secondary source (De Beers, unpub. data, 1978, 1984). Rounding and abrasion of some indicator minerals reflect reworking and sorting of grains in the extensive panneveld environment (Rio Tinto Namibia, unpub. data., 1995). The overlying Kalahari units reflect alternating wet and dry conditions (Albat, 1978). The present surface consists of wind-blown sand, dunes, and thick layers of calcrete, silcrete, and ferricrete in the vicinity of pan areas.

Geochemistry

Methodology

The garnets used in this study come from the Tsumkwe area (Fig. 1B) and represent kimberlite indicator minerals collected by Rio Tinto from a wider region over the course of exploration (1994 to 1996). The grains chosen for analysis are chemically and geographically representative of the larger garnet indicator mineral population, consisting of a few hundred garnets of which approximately 20 percent are subcalcic G10 garnets. The garnets were mounted in epoxy and analyzed by electron microprobe for major elements by Scientific Services, Cape Town at the Department of Geological Sciences, University of Cape Town.

Garnets on one polished disk were subsequently analyzed by proton microprobe for trace elements in the CSIRO Division of Exploration and Mining, North Ryde. Methods used are described in detail by Griffin *et al.* (1988, 1989) and Ryan *et al.* (1990a, b). The pro-

Table 1: Compositions and T_{Ni}°C of Indicator Mineral Garnets from the Tsumkwe Region

Grain no.	1	2	3	4	5	6	7	8	9	10	11	12
Cr_2O_3 wt %	2.20	2.15	6.32	7.35	2.82	3.61	3.03	6.20	4.34	5.20	9.99	3.98
TiO_2	0.100	0.120	0.100	0.100	0.100	0.260	0.190	0.100	0.100	0.100	0.100	0.100
FeO	9.43	9.30	6.52	7.04	8.83	8.35	7.39	6.75	8.65	7.25	5.61	8.42
CaO	4.69	4.83	3.08	6.62	5.33	5.01	4.56	6.03	5.78	5.47	3.12	5.08
Ni ppm	23.1	17.4	61.4	43.2	10.7	43.5	46.8	51.4	26.5	31.2	57.8	22.4
Zn	9.85	9.53	11.10	11.50	6.51	9.21	8.47	9.22	8.81	12.10	12.20	8.49
Ga	7.38	4.82	5.72	5.74	5.02	10.60	5.60	4.02	9.31	7.90	6.68	5.98
Sr		0.295	3.24	2.16	1.18	1.00	0.08401	1.02	0.229	1.08	1.32	
Y	9.96	13.20	3.57	1.83	25.70	26.20	11.80	6.14	8.45	9.44	2.90	14.10
Zr	1.40	7.07	18.60	9.44	21.00	54.40	29.20	63.10		90.50	16.60	42.90
T_{Ni}°C	826 ± 56.7	765 ± 39.5	1109 ± 48.6	992 ± 41.8	674 ± 51.1	994 ± 41	1017 ± 38.7	1047 ± 44.3	859 ± 46.3	900 ± 42.6	1087 ± 42.4	819 ± 52.4
Grain no.	13	14	15	16	17	18	19	20	21	22	23	24
Cr_2O_3 wt %	1.78	2.6	2.49	2.43	2.92	0.244	3.33	6.64	2.98	5.84	5.56	4.04
TiO_2	0.550	0.220	0.100	0.100	0.200	1.110	0.100	0.100	0.100	0.240	0.180	0.100
FeO	7.69	11.60	8.60	9.25	7.44	10.90	9.06	5.98	9.45	7.74	8.69	8.55
CaO	4.86	4.80	5.38	5.27	4.23	4.84	5.59	2.70	5.37	5.31	5.89	5.02
Ni ppm	69.8	39.7	7.35	10.1	30.1	40.2	13.8	41.4	16.8	40.9	37.3	23.8
Zn	11.90	18.70	5.93	5.86	8.55	20.40	7.70	10.30	9.54	10.20	11.40	10.40
Ga	10.50	10.90	4.07	3.75	8.17	20.20	7.08	2.86	7.24	6.74	9.31	5.14
Sr	0.221	0.352	1.030		0.691	0.511	1.190	6.080		0.05089		0.321
Y	19.70	15.90	1.43	5.11	16.90	31.10	16.6	1.76	17.60	29.40	12.80	12.50
Zr	54.70	34.60	5.81	14.40	42.50	177.00	15.4	16.60	9.80	153.00	75.60	40.60
T_{Ni}°C	1157 ± 42.9	967 ± 37.5	614 <	664 ± 51.3	891 ± 36.2	971 ± 48.7	720 ± 61.6	979 ± 37.8	759 ± 40	976 ± 44.7	949 ± 40.6	833 ± 38.6
Grain no.	25	26	27	29	30	31	32	33	34	35	36	37
Cr_2O_3 wt %	4.15	4.31	2.61	2.54	3.03	2.24	2.87	4.08	3.56	2.65	3.30	6.10
TiO_2	0.320	0.260	0.150	0.100	0.100	0.100	0.100	0.160	0.250	0.100	0.100	0.100
FeO	6.57	8.27	7.90	9.15	9.95	9.26	8.83	5.73	7.77	9.55	8.75	5.81
CaO	4.73	4.97	4.60	5.54	5.11	5.23	5.16	4.86	4.84	4.88	5.48	3.38
Ni ppm	59.2	35.1	52.2	14.6	20.7	10.7	12.5	86.4	52.3	21.2	13.4	64.9
Zn	11.70	11.10	13.00	5.23	11.40	10.00	5.50	12.60	9.66	8.13	6.15	8.78
Ga	11.30	9.82	8.90	2.08	6.36	5.73	3.57	4.55	7.92	3.73	3.99	6.40
Sr	0.625	1.020	0.326	0.594			0.405	0.112		0.748		1.810
Y	11.70	21.50	13.70	4.52	10.00	21.60	20.60	3.01	34.80	11.50	35.80	6.66
Zr	27.30	63.20	21.70	36.60	5.03	12.90	74.40	19.90	145.00	27.80	79.00	27.20
T_{Ni}°C	1096 ± 40.4	932 ± 41.7	1052 ± 41.1	730 ± 70.1	802 ± 39.3	675 ± 59.5	701 ± 50.6	1245 ± 49.5	1053 ± 39.7	807 ± 46.3	714 ± 43.9	1129 ± 42.9
Grain no.	38	39	40	41	42	43	44	45	46	47	48	49
Cr_2O_3 wt %	2.89	5.13	3.46	2.43	3.51	2.37	5.19	3.94	6.00	6.42	5.78	4.26
TiO_2	0.100	1.520	0.100	0.400	0.100	0.100	0.100	0.100	0.130	0.100	0.100	0.290
FeO	8.71	9.45	7.96	8.07	7.48	7.59	7.07	7.29	7.19	6.35	6.54	7.79
CaO	5.14	4.69	4.38	3.70	4.24	3.84	5.17	5.10	5.23	4.00	5.16	4.92
Ni ppm	9.43	11.4	20.6	63.9	36.8	53.6	29.2	35.1	28.1	43.3	58.4	39.4
Zn	6.40	6.95	8.13	12.60	8.55	12.10	8.70	8.67	9.27	10.70	11.50	12.10
Ga	4.82	7.15	3.96	12.90	4.79	7.68	2.96	4.69	3.36	5.03	5.32	9.92
Sr			0.328		0.09816			1.340		1.240	0.375	1.380
Y	20.00	24.00	35.30	19.50	4.17	10.10	4.01	4.74	15.90	2.50	7.31	14.70
Zr	27.40	9.71	31.00	44.40	81.20	10.80	58.30	41.20	64.00	18.90	33.20	73.10
T_{Ni}°C	653 ± 55.4	685 ± 47.3	801 ± 48.3	1124 ± 45.3	945 ± 40	1061 ± 39.5	883 ± 48	932 ± 42.6	873 ± 43	993 ± 43.9	1091 ± 41	965 ± 37.4

Notes: Uncertainties for T_{Ni}°C are given at the one sigma level; full major-element compositional data for the garnets are on Open File at the Geological Survey of Namibia

ton microprobe provides a beam of 3 MeV protons that is focused onto a sample by an electrostatic lens (Sie and Ryan, 1986). The characteristic X-rays generated by the proton bombardment are collected by a Si (Li) energy-dispersive detector and displayed as spectra. The typical size of the beam spot on the sample is 30 microns, and beam currents are 10 to 15 nA. Counting times correspond to analysis times of 4 to 6 minutes per sample. Methods for interpreting the trace element data, and for deriving T_{Ni}, P_{Cr}, and depth of lithosphere, are described by Griffin and Ryan (1995) and Ryan *et al.* (1996).

Results

Results for 49 mantle garnets are presented in Table 1. As a consequence of their representing a fairly widely distributed loam sample population, the garnets show some anticipated spread in their trace element compositions. This spread is illustrated in the distribution of the garnets on a P_{Cr} versus T_{Ni} diagram (Fig. 2), which also shows a range of model conductive geotherms (Pollack and Chapman, 1977). In this plot, the geotherm is defined by the envelope of maximum P_{Cr} at each T_{Ni} (Ryan *et al.*, 1996). Most of the garnets are consistent with derivation from a mantle with a geotherm close

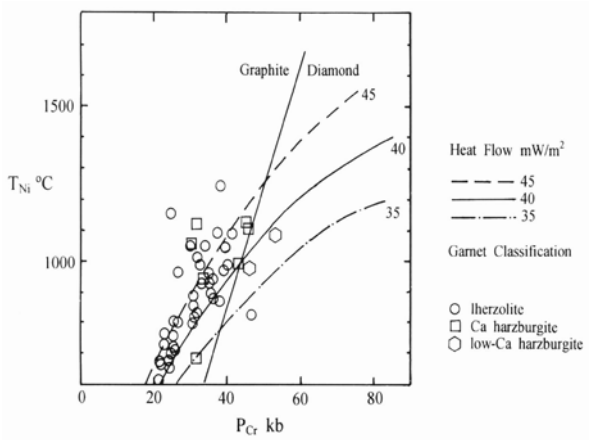

Figure 2: Plot of P_{Cr} (kb) versus T_{Ni}°C for indicator mineral garnets from the Tsumkwe region, illustrating a garnet geotherm close to 40 mW/m², a diamond window between 900° and 1250°C, and an implied lithosphere thickness of approximately 190 km.

to the model corresponding to a surface heat flow of 40 mW/m², which is typical of cratonic mantle, while some garnets indicate derivation from a mantle with a cooler geotherm of approximately 35 to 38 mW/m². Thus, a range in possible mantle conditions is represented by the regionally sampled garnets, in keeping with the wide distribution of the sample sites. The estimated thickness of the lithosphere is derived from the highest temperature at which depleted (Y-poor) garnets occur (1250°C). In this sample set, such garnets occur up to the highest temperatures found (1250°C), indicating a lithosphere at least 190 km thick. The diamond window, or range of temperatures compatible with diamond formation for this sample population, is defined by the temperature interval from the intersection of the geotherm with the diamond-graphite curve to the base of the sampled lithosphere (from 900° to 1250°C; Fig. 2). The peak in the number of garnets analyzed falls within this diamond window (Fig. 3).

In this representative sample population, there are five G10 (Cr-rich, subcalcic) garnets. By analogy with

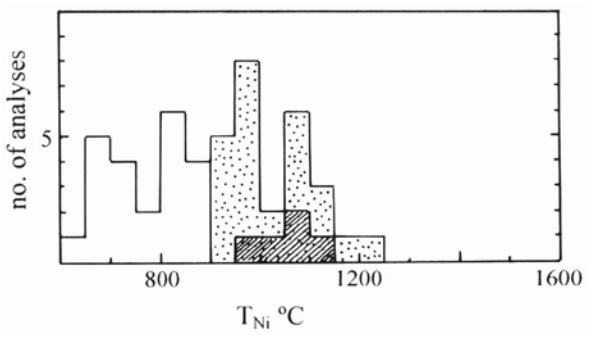

Figure 3: Histogram showing temperatures (T_{Ni}°C) determined for indicator mineral garnets from the Tsumkwe region. The stippled pattern represents garnets in the diamond window, and the hatchured pattern represents the five G10 garnets in the representative sample population.

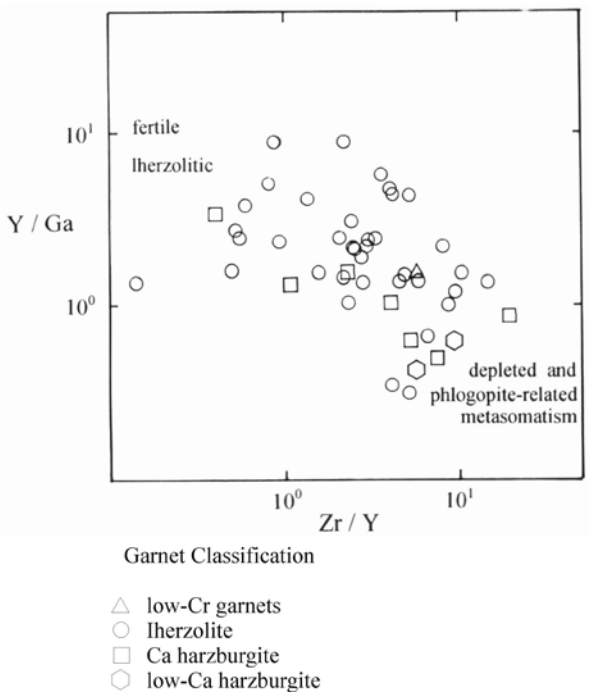

Figure 4: Plot of Zr/Y versus Y/Ga in indicator mineral garnets from the Tsumkwe region, illustrating the range in metasomatic mantle garnet compositions represented by the sample population.

diamond-inclusion garnets, these garnets are presumably derived from depleted harzburgitic mantle (Gurney and Zweistra, 1995). The G10 garnets plot within the diamond window for northeast Namibia (Fig. 3), indicating the presence of potentially diamondiferous, depleted mantle beneath that region at the time of entrainment to the surface. These garnets also have depleted compositions with respect to trace elements (notably Zr, Y and Ti), indicating that diamond-destructive melt metasomatism (Griffin and Ryan, 1995) did not affect this segment of the mantle. Phlogopite-related metasomatism, which is characteristic of xenoliths from much of the Kaapvaal craton, dominates the metasomatic style of the remainder of the garnets and is represented by relatively high Zr/Y and low Y/Ga values (Fig. 4). Higher Y/Ga in some garnets may reflect derivation from relatively fertile garnet lherozolites more typical of Proterozoic mantle (Griffin *et al.*, 1998). These observations underscore the probability that the spread of trace element compositions represented by the sample population (Fig. 4) reflects the range of possible mantle sources for the group as a whole.

Geochronology

Methodology

Samples of basement megacrystic granite and fine-grained granitic gneiss were collected from the eastern part of the Tsumkwe area, in the vicinity of the Ju/”hoansi settlement at Makuri Vlei, where the Kalahari cover is

Table 2: Summary of SHRIMP U-Th-Pb zircon results for the megacrystic granite

Grain. Spot	U (ppm)	Th (ppm)	Th/U	Pb* (ppm)	$^{204}Pb/^{206}Pb$	f_{206} %	Measured ratios $^{206}Pb/^{238}U$	±	$^{207}Pb/^{206}U$	±	Radiogenic $^{206}Pb/^{235}U$	±	Age (Ma) $^{206}Pb/^{238}Pb$	±
1.1	85	84	0.99	14	0.002710	4.21	0.1479	0.0041	0.1013	0.0023	0.1417	0.0039	854	22
2.1	121	138	1.14	21	0.000704	2.11	0.1474	0.0040	0.0840	0.0017	0.1442	0.0039	869	22
3.1	423	457	1.08	70	0.001182	1.80	0.1420	0.0031	0.0814	0.0009	0.1394	0.0031	841	17
4.1	253	199	0.79	41	0.001129	1.67	0.1466	0.0038	0.0803	0.0013	0.1442	0.0038	868	21
5.1	82	134	1.63	16	0.002601	3.16	0.1482	0.0051	0.0926	0.0020	0.1435	0.0049	864	28
6.1	264	287	1.09	45	0.000965	1.17	0.1442	0.0036	0.0761	0.0008	0.1425	0.0036	859	20
7.1	101	118	1.17	17	0.000744	1.55	0.1390	0.0037	0.0793	0.0013	0.1369	0.0037	827	21
8.1	227	283	1.24	39	0.000301	0.69	0.1393	0.0031	0.0722	0.0011	0.1383	0.0031	835	18
9.1	43	45	1.04	7	0.001097	2.55	0.1409	0.0044	0.0876	0.0022	0.1374	0.0043	830	24
10.1	316	381	1.21	56	0.000123	0.34	0.1430	0.0032	0.0692	0.0004	0.1425	0.0032	859	18
11.1	62	67	1.08	11	0.000440	1.71	0.1447	0.0039	0.0806	0.0018	0.1422	0.0038	857	22
12.1	121	138	1.14	21	0.000558	1.08	0.1445	0.0037	0.0754	0.0007	0.1430	0.0036	861	21
13.1	292	301	1.03	50	0.001371	2.02	0.1452	0.0040	0.0832	0.0008	0.1423	0.0039	857	22

Notes: 1. Uncertainties given at the one σ level; 2. $f206$ % donates the percentage of ^{206}Pb that is common Pb. 3. Correction for common Pb made use the measured $^{238}U/^{206}Pb$ and $^{207}Pb/^{206}Pb$ ratios following Terra and Wasserburg (1972) as outlined in Compston *et al.* (1992).

thin to nonexistent (Fig. 1B). The gneissic sample is considered to represent the major geologic map unit (Mgr) as identified on the 1:1 000 000 Geological Map of Namibia (1980). Likewise, the megacrystic granite appears to be widespread and similar rocks exposed on the Botswana side of the border (J. Green, pers. comm., 1995) may be part of the same complex. After cleaning and chipping, approximately 2 kg of each rock type were then crushed and zircons were removed using standard heavy liquid and magnetic techniques. Representative zircons from each sample were mounted in epoxy with standard zircon SL13, sectioned, and polished. They were analyzed by ion microprobe on SHRIMP 1 at the Australian National University. The SL13 standard was analyzed 13 times in the session.

The data were reduced in a manner similar to that of Compston *et al.* (1992) and the analyses consisted of six scans through the mass range. The Pb/U ratio was normalized to a value of 0.0928 for the $^{206}Pb/^{238}U$ ratio for this standard, i.e., equivalent to an age of 672 Ma. For the megacrystic granite, the correction for common lead was made using the measured $^{207}Pb/^{206}Pb$ and $^{238}U/^{206}Pb$ ratios following Tera and Wasserburg (1972) as described in Compston *et al.* (1992). For the granitic gneiss, the common lead corrections were made using the directly measured abundances of ^{204}Pb and the appropriate compositions according to the Cumming and Richards (1975) model. Uncertainties in the isotopic ratios and ages in the data tables (and in the error bars in the plotted data) are reported at the 1 sigma level, but final ages on pooled data are reported as weighted means with 95% confidence limits. All age calculations and statistical assessments of the data have been done utilizing the geochronological statistical software package Isoplot/Ex (version 2.00) of Ludwig (1999).

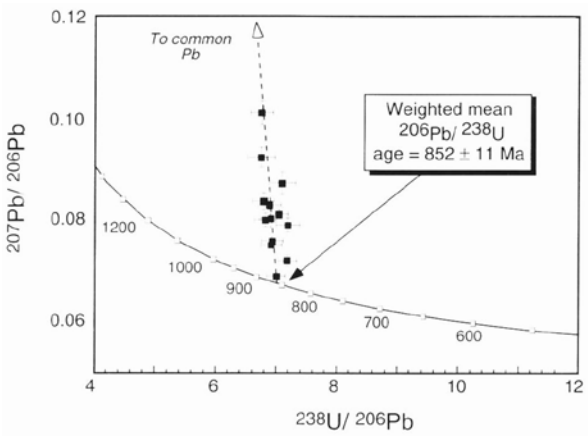

Figure 5: Tera-Wasserburg plot of U-Pb SHRIMP data for megacrystic granite from the Tsumkwe region. Error bars represent one sigma uncertainty. The Concordia curve is calibrated in Ma.

Results

Zircons in the megacrystic granite are well preserved despite the weathered nature of the sample. They comprise a single population of euhedral, clear magmatic grains ranging from colorless to a light ginger color. Subtle magmatic zoning is discernible in some grains in thin section. The chemistry of the zircons is also uniform, with little variation in Th/U ratios although the concentrations of both U and Th vary significantly from grain to grain. Thirteen analyses were carried out on 13 grains (Table 2). All of the data points plot in a linear array in the Tera-Wasserburg plot of uncorrected (for common Pb) data (Fig. 5). Statistically, all 13 analyses are of the same age, with the weighted mean $^{206}Pb/^{238}U$ age calculated at 852 ± 11 Ma (MSWD = 0.46; probability = 0.94; uncertainty quoted at the 95% confidence level from s_{obs}).

Zircons from the fine-grained granitic gneiss show an almost complete lack of idiomorphism. They are generally dark brown to reddish brown and appear to have

Table 3: Summary of SHRIMP U-Th-Pb zircon results for the fine-grained granitic gneiss

Grain.	U	Th	Th/U	Pb*	$^{204}Pb/$	f_{206}	Radiogenic Ratios						Ages (in Ma)						Conc.
Spot	(ppm)	(ppm)		(ppm)	^{206}Pb	%	$^{206}Pb/^{238}U$	±	$^{207}Pb/^{235}U$	±	$^{207}Pb/^{206}Pb$	±	$^{206}Pb/^{238}Pb$	±	$^{207}Pb/^{235}U$	±	$^{207}Pb/^{206}U$	±	%
1.1	638	201	0.32	189	0.000148	0.23	0.2820	0.0067	4.420	0.122	0.1137	0.0013	1601	34	1716	23	1859	20	86
2.1	556	57	0.10	154	0.000071	0.11	0.2781	0.0078	4.556	0.157	0.1188	0.0020	1582	40	1741	29	1939	30	82
3.1	865	446	0.52	294	0.000396	0.61	0.3071	0.0065	4.814	0.110	0.1137	0.0007	1727	32	1787	19	1859	12	93
4.1	511	338	0.66	194	0.000094	0.15	0.3326	0.0075	5.563	0.136	0.1213	0.0008	1851	37	1910	21	1975	12	94
5.1	623	261	0.42	209	0.000188	0.29	0.3079	0.0070	4.947	0.120	0.1165	0.0007	1731	35	1810	21	1904	11	91
6.1	539	187	0.35	154	0.000157	0.24	0.2663	0.0056	4.206	0.097	0.1145	0.0008	1522	29	1675	19	1873	13	81
7.1	1276	1265	0.99	558	0.000090	0.14	0.3585	0.0094	6.139	0.171	0.1242	0.0009	1975	45	1996	25	2017	13	98
7.2	623	186	0.30	178	0.000106	0.16	0.2713	0.0058	4.346	0.107	0.1162	0.0012	1548	29	1702	21	1898	18	82
8.1	764	349	0.46	223	0.000197	0.30	0.2640	0.0056	3.944	0.091	0.1084	0.0008	1510	28	1623	19	1772	13	85
10.1	824	467	0.57	282	0.000069	0.11	0.3042	0.0067	4.979	0.117	0.1187	0.0007	1712	33	1816	20	1937	11	88
11.1	585	267	0.46	122	0.000142	0.22	0.1900	0.0040	2.981	0.069	0.1138	0.0008	1122	22	1403	18	1860	13	60
12.1	608	316	0.52	205	0.000124	0.19	0.3031	0.0066	5.133	0.120	0.1228	0.0007	1706	33	1842	20	1998	11	85
12.2	891	169	0.19	194	0.000381	0.58	0.2102	0.0045	3.191	0.075	0.1101	0.0008	1230	24	1455	18	1801	14	68
13.1	798	317	0.40	188	0.000137	0.21	0.2148	0.0072	3.276	0.115	0.1106	0.0007	1255	38	1475	28	1809	12	69
14.1	964	76	0.08	145	0.000128	0.20	0.1602	0.0033	1.583	0.038	0.0717	0.0007	958	18	963	15	976	19	98
15.1	1070	1177	1.10	481	0.000034	0.05	0.3632	0.0134	6.246	0.236	0.1247	0.0007	1997	64	2011	34	2025	10	99
16.1	1913	1661	0.87	560	0.000032	0.05	0.2476	0.0051	3.919	0.084	0.1148	0.0005	1426	26	1618	18	1877	8	76
17.1	1275	495	0.39	327	0.002117	3.24	0.2327	0.0155	3.759	0.264	0.1171	0.0018	1349	82	1584	58	1913	28	71

Notes: 1. Uncertainties given at the one σ level; 2. f206 % denotes the percentage of ^{206}Pb that is common Pb. 3. Correction for common Pb made using the measured $^{204}Pb/^{206}Pb$ ratios. 4. For % Conc., 100% denotes a concordant analysis.

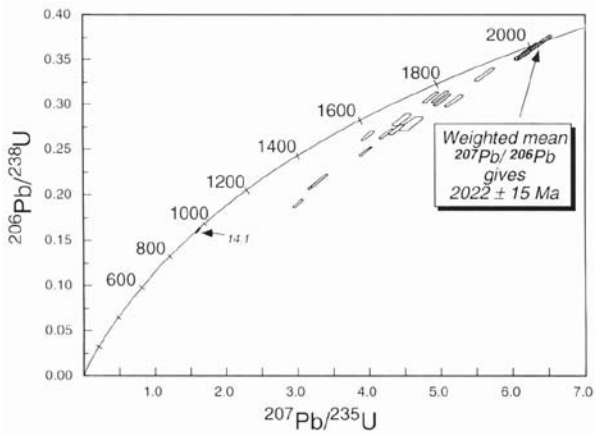

Figure 6: U-Pb Concordia diagram for SHRIMP data for granitic gneiss from the Tsumkwe region.

suffered some radiation damage. Some grains are small aggregates of crystals, possibly resulting from instability and resorption during a metamorphic event. Other grains retain original igneous textures such as compositional zoning. Eighteen analyses on 16 zircon grains (Table 3) produced some scatter and complexity of data (Fig. 6). Most analyses are highly discordant, falling in a broad band with a trend that suggests significant nonzero-age lead loss. This complicates establishment of an age, the best estimate for which comes from the two concordant analyses 7.1 and 15.1 (Table 3). The weighted mean $^{207}Pb/^{206}Pb$ age for these two points is 2022 ± 15 Ma. A single analysis (14.1, Table 3) plots close to the concordia at about 970 Ma and may reflect Pb loss or metamorphism at this time. Support for a metamorphic origin may be indicated by the relatively low Th and Th/U of this grain.

Discussion

The emplacement age of 852 ±11 Ma for the megacrystic granite in the study area is relatively old compared to the 756 ± 2 Ma Oas quartz syenite complex that represents the approximate beginning of Pan-African sedimentation in northwest Namibia (Hoffman *et al.*, 1996). However, the temporal coincidence between the 852 Ma date obtained and 880 to 820 Ma zircon ages reported for basal metarhyolite and syntectonic granite in the Zambezi belt in Zambia (Hanson *et al.*, 1994) suggest contemporaneous magmatic activity. The megacrystic granite in the Tsumkwe region could be associated with closure of the Zambezi belt, thus predating the earliest stage of continental breakup on the north side of the Khomas ocean at ca. 757 Ma (Hoffman *et al.*, 1996).

The 2022 ± 15 Ma age obtained for basement rocks in the Tsumkwe region is similar to ages that are typical of the Kheis-Magondi belt, which wraps around the Kaapvaal craton. Correspondingly, it is surmised that the basement complex in the study area forms part of a belt of Proterozoic age that encompasses the Congo craton. The single near-concordant analysis of about 970 Ma for the gneiss may reflect metamorphism approximately contemporaneous with the broad thermal event that occurred in the Namaqua orogeny after the peak of granulite metamorphism. This event could therefore be associated with the northeast-trending Kibaran (1.3-1.0 Ga) Namaqua-Irumide belt that extends into Zambia.

It has been postulated that the southern Congo craton is defined by ca. 2.7 Ga Archean gneisses that extend southward into Namibia from Angola (Carvalho and

Alves, 1993). The age of the craton in northwest Namibia is supported by recent U-Pb zircon analyses that yielded ages of 2645 ± 6 Ma (Seth *et al.*, 1997, 1998) and ca. 2620 Ma (Franz *et al.*, 1999) for gneissic basement in the Kaoko belt. Sm-Nd isotope data indicate that even older crustal material was involved in the formation of these gneisses (Seth *et al.*, 1998). This Archean basement was intruded by 1961 ± 4 Ma granodiorite (U-Pb single zircon; Seth *et al.*, 1997, 1998), an age that is broadly similar to the 2022 ± 15 Ma emplacement age obtained for the fine-grained gneiss in the Tsumkwe region. Both ages are significantly older than the inferred 1800 Ma for the Grootfontein complex, to which the Tsumkwe unit has been assigned previously (Balfour *et al.*, 1985). Attempts at directly correlating pre-Damara basement complexes that underlie the Kaoko belt and the Tsumkwe region are difficult in view of the intervening thick cover of Kalahari sediments. However, a comparison may be made between this mid-Proterozoic circum-Congo belt and the equivalent Kheis-Magondi belt around the Kaapvaal craton. There, Nd model ages of ca. 2.5 to 3.0 Ga (Harris *et al.*, 1987) indicate the presence of an ancient crustal component occurring in a circumcratonic belt. Despite the garnet geochemical evidence cited above for Archean-like depleted mantle beneath the Tsumkwe area, to date no evidence of an Archean component has been produced from apparent zircon cores analyzed from the 2022 Ma gneiss. Further work is needed to resolve this question.

The results of this study indicate the presence of a continental segment in the region of northeast Namibia that was established by at least 2.02 Ga. Subcalcic garnets are relatively rare in terranes with juvenile Proterozoic crust, compared to Archean crust, but they are found where Archean crust has been reworked during the Proterozoic (Griffin *et al.*, 1998). For the Tsumkwe area, the occurrence of mantle garnets with geochemical signatures indicating derivation from a thick, depleted lherzolite-harzburgite lithosphere with a significant diamond window suggests a component of Archean-like cratonic mantle lithosphere at depth. However, many garnets analyzed also indicate derivation from relatively fertile lithospheric mantle. This combination of geochemical styles is similar to that observed for mantle-derived xenoliths and garnets from the Gibeon area (Hoal *et al.*, 1995). There, garnets with cratonic metasomatic signatures and xenoliths with compositions intermediate between cratonic and oceanic lithosphere reflect the transitional nature of the lithosphere beneath the Kheis-Magondi and related Proterozoic belts around the Kaapvaal craton. The intermediate-composition lithosphere has been interpreted to contain remnants of reworked Archean lithosphere combined with basaltic underplating, supported by the extensional nature of the western margin of the Kaapvaal craton derived from seismic profiles (Hoal *et al.*, 1995). Some Botswana kimberlites occur in a tectonic setting similar to the Gibeon region in that they occur in a hybrid zone of Archean and Proterozoic crustal components marginal to the Archean Zimbabwe craton (Fig. 1A). By analogy to the Gibeon area (Kaapvaal craton edge) and to the Botswana kimberlites (Zimbabwe craton edge), the cratonic segment underlying the Tsumkwe area may have been a thinned lithospheric edge of the Congo craton. The phenomenon of retention of cratonic lithosphere in circumcratonic belts may therefore be more widespread than previously recognized.

Acknowledgments

The results reported in this paper constitute information gained while the first author was an employee with Rio Tinto Namibia. We are particularly grateful to Kevin Fox (Rio Tinto) for permission to publish these data, and to John Collier (Rio Tinto) and Ken Hart (formerly Rio Tinto Namibia) for committing to the study in 1995. The Geological Survey of Namibia provided assistance in research conducted in 1994 and 1995 on kimberlites and the tectonic setting of regions surrounding the Kaapvaal craton. Chris Ryan and Tin Tin Win provided invaluable assistance with the proton microprobe analyses. Craig Smith and Bruce Eglington provided valuable reviews of the manuscript.

References

Albat, H. 1978. The geology of the Kalahari beds of northeastern S.W.A. *Unpubl. Rep. De Beers Prospecting S.W.A*.

Balfour, D.J., Hegenberger, W., Medlycott, A.S. and Wilson, K.J. 1985. Kimberlites near Sikereti, northeastern South West Africa/Namibia. *Communs geol. Surv. S.W. Afr./Namibia*, **1**, 69-77.

Carvalho, H. de and Alves, P. 1993. The Precambrian of SW Angola and NW Namibia. *Comunicações, Instituto de Investigação Científica Tropical, Série de Ciências da Terra, Lisboa*, **4**, 38 pp.

Compston, W., Williams, I.S., Kirschvink, J.L., Zhang Zichao and Guogan, M.A. 1992. Zircon ages for the Early Cambrian time scale. *J. geol. Soc. Lond.*, **149**, 171-184.

Cumming, G.L. and Richards, J.R. 1975. Ore lead isotope ratios in a continuously changing Earth. *Earth Planet. Sci. Lett.*, **28**, 155-171.

Eberle, D., Andritsky, G. and Wackerle, R. 1995. The new magnetic data set of Namibia: Its contributions to the understanding of crustal evolution and regional distribution of mineralization. *Communs geol. Surv. Namibia*, **10**, 141-150.

Franz, L., Romer, R.L. and Dingeldey, D.P. 1999. Diachronous Pan-African granulite-facies metamorphism (650 and 55 Ma) in the Kaoko belt, NW Namibia. *Eur. J. Mineral.*, **11**, 167-180.

Geological Map of Namibia. 1980. Scale 1: 1 000 000. *Geol. Surv. Namibia* (reprinted 1990).

Griffin, W.L. and Ryan, C.G. 1995. Trace elements in

indicator minerals: Area selection and target evaluation in diamond exploration. *J. geochem. Explor*., **53**, 311-337.

Griffin, W.L., Jaques, A.L., Sie, S.H., Ryan, C.G., Cousens, D.R. and Suter, G.F. 1988. Conditions of diamond growth: A proton microprobe study of inclusions in West Australian diamonds. *Contrib. Mineral. Petrol.*, **99**, 143-158.

Griffin, W.L., Smith, D., Boyd, F.R., Cousens, D.R., Ryan, C.G., Sie, S.H. and Suter, G.F. 1989. Trace element zoning in garnets from sheared mantle xenoliths. *Geochim. Cosmochim. Acta*, **53**, 561-567.

Griffin, W.L., O'Reilly, S.Y., Ryan, C.G., Gaul, O. and Ionov, D. 1998. Secular variation in the composition of subcontinental lithospheric mantle. *In*: Braun, J., Dooley, J.C., Goleby, B.R., van der Hilst, R.D. and Klootwijk, C.T. (eds) *Structure and evolution of the Australian continent*; *Geodynamics*, **26**, Amer. Geophys. Union, Washington D.C., 1-26.

Gurney, J.J. and Zweistra, P. 1995. The interpretation of the major element compositions of mantle minerals in diamond exploration. *In*: Griffin, W.L. (ed.) *Diamond exploration: Into the 21st century*. J. geochem. Explor., **53**, 293-309.

Hanson, R.E., Bowring, S.A., Wardlaw, M.S. and Wilson, T.J. 1994. Intracontinental origin of the Pan-African Zambezi orogenic belt, Zambia, in relation to the regional Proterozoic tectonic framework of southern Africa. *Abstracts, Conference on Proterozoic Crustal and Metallogenic Evolution, Windhoek, Geol. Soc. and Geol. Surv. Namibia*, **24**.

Harris, N.B.W., Hawkesworth, C.J., Van Calsteren, P. and McDermott, F. 1987. Evolution of continental crust in southern Africa. *Earth Planet. Sci. Lett*., **83**, 85-93.

Hoal, B.G., Hoal, K.E.O., Boyd, F.R. and Pearson, D.G. 1995. Age constraints on crustal and mantle lithosphere beneath the Gibeon kimberlite field, Namibia. *S. Afr. J. Geol*., **98**, 112-118.

Hoffman, P.F., Hawkins, D.P., Isachsen, C.E., and Bowring, S.A. 1996. Precise U-Pb zircon ages for early Damaran magmatism in the Summas Mountains and Welwitschia Inlier, northern Damara belt, Namibia. *Communs geol. Surv. Namibia*, **11**, 47-52.

Ludwig, K.R. 1999. Isoplot/Ex version 2.00: A geochronological toolkit for Microsoft Excel. *Spec. Publ. Berkeley Geochronology Center*, **1a**, 46 pp.

Pollack, H.N. and Chapman, D.S. 1977. On the regional variation of heat flow, geotherms and lithospheric thickness. *Tectonophys*., **38**, 279-296.

Ryan, C.G., Cousens, D.R., Sie, S.H., Griffin, W.L. and Suter, G.F. 1990a. Quantitative PIXE microanalysis of geological material using the CSIRO proton microprobe. *Nucl. Instrum. Meth*., **B47**, 55-71.

Ryan, C.G., Cousens, D.R., Sie, S.H. and Griffin, W.L. 1990b. Quantitative analysis of PIXE spectra in geoscience applications. *Nucl. Instrum. Meth.*, **B49**, 271-276.

Ryan, C.G., Griffin, W.L. and Pearson, N.J. 1996. Garnet geotherms: A technique for derivation of P-T data from Cr-pyrope garnets. *J. geophys. Res.*, **101**, 5611-5625.

Seth, B., Kröner, A., Dürr, S.B., Dingeldey, D.P. and Okrusch, M. 1997. Archean terrane identification and late Pan-African metamorphism in the Kaoko belt, Namibia: Significance for Gondwana assembly. *Abstract Supplement No. 1, EUG meeting, Strasbourg, Terra Nova*, **9**, 168.

Seth, B., Kröner, A., Mezger, K., Nemchin, A.A., Pidgeon, R.T. and Okrusch, M. 1998. Archaean to Neoproterozoic magmatic events in the Kaoko belt of NW Namibia and their geodynamic significance. *Precambr. Res.*, **92**, 341-363.

Sie, S.H. and Ryan, C.G. 1986. An electrostatic "Russian" quadruplet microprobe lens. *Nucl. Instrum. Meth.*, **B15**, 664-668.

Tera, F. and Wasserburg, G.J. 1972. U-Th-Pb systematics in three Apollo 14 basalts and the problem of initial Pb in lunar rocks. *Earth Planet. Sci. Lett*., **14**, 281-304.

Uken, R. and Watkeys, M.K. 1997. An interpretation of mafic dyke swarms and their relationship with major mafic magmatic events on the Kaapvaal craton and Limpopo belt. *S. Afr. J. Geol.*, **100**, 341-348.